A

BIOLOGICAL SAMPLES
44 male surgical GBM specimens
32 female surgical GBM specimens

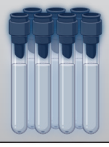

DATA ACQUISITION
LC/MS and GS/MS[S1],[S2]

DATA PROCESSING AND ANALYSIS
1. Metabolite identification through reference library (757 metabolites)[S1]
2. Data normalization[S1]
3. Removal of metabolites constant across samples (718 metabolites)
4. $\log_2$-transformation and z-score calculation for each metabolite

DATA PRESENTATION

Super-pathway analysis (Fig. 1A)
1. Divide metabolites into super-pathways and average z-scores
2. Calculate male/female $\log_2$ fold-change

Sub-pathway analysis (Fig. 1B)
1. Divide metabolites into sub-pathways and average z-scores
2. Calculate male/female $\log_2$ fold-change

Individual metabolite analysis (Fig. 1C-D)
1. Select top 75 metabolites (greatest mean difference between male and female samples)
2. Create metabolite clusters and heatmap

B

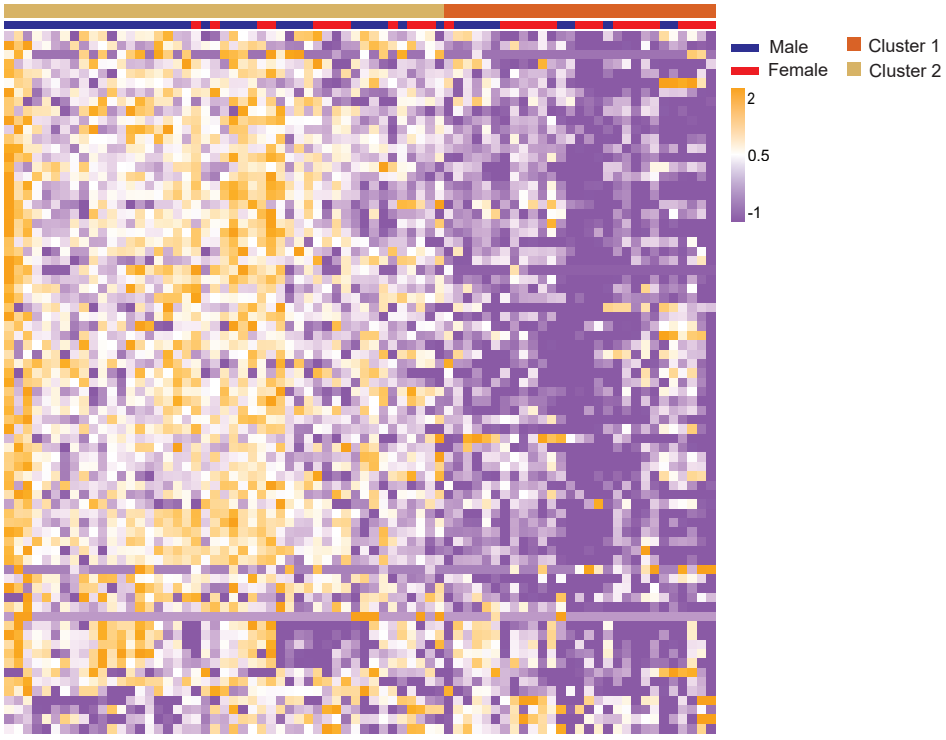

C

	Cluster 1 = low metabolite abundance	Cluster 2 = high metabolite abundance
Male	10	34
Female	19	13

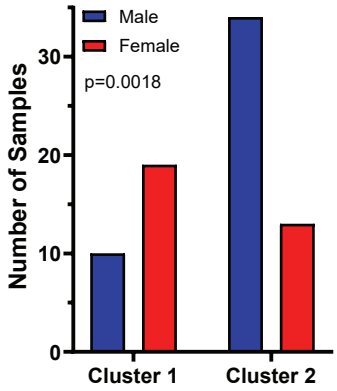

Figure S1. Sex differences in GBM metabolite abundance parallel those found in serum, related to Figure 1 A, Workflow of the methodology of data collection, analysis, and presentation of the human GBM surgical specimens. **B,** K-means clustering (n=2) of the top 75 metabolites (determined by greatest mean difference) of male (n=44) and female (n=32) GBM surgical specimens. Patient specimens and metabolites are represented in columns and rows, respectively. Cluster 1 represents the low metabolite abundance group; cluster 2 represents the high metabolite abundance group. **C,** Male and female tumor sample distribution in cluster 1 and cluster 2. ***p=0.0018; two-tailed Fisher's exact test.

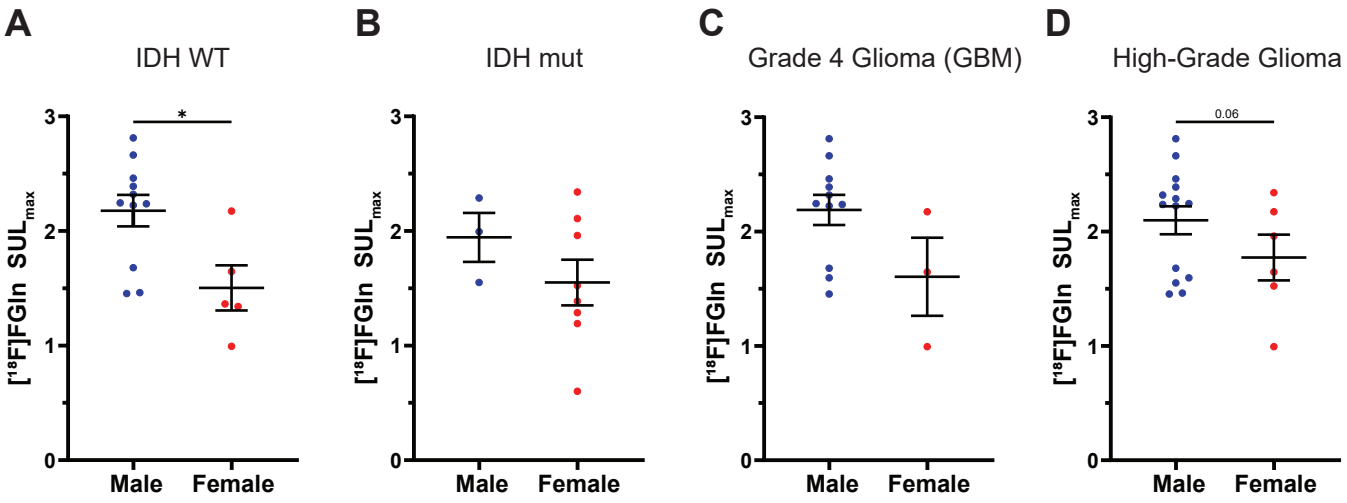

Figure S2. Glutamine uptake in male and female patient glioma subsets, related to Figure 2

A-D, Quantification of [^{18}F]FGln uptake in male and female IDH wild-type (WT) gliomas (**A**), IDH mutant (mut) gliomas (**B**), grade 4 gliomas (GBM) (**C**), and high-grade gliomas (HGG) (**D**) (SULmax). Data are mean +/- SEM of n=11 male and n=5 female IDH WT patients, n=3 male and n=8 female IDH mutant patients, n=11 male and n=3 female GBM, and n=14 male and n=6 female HGG. *p<0.05; t-test.

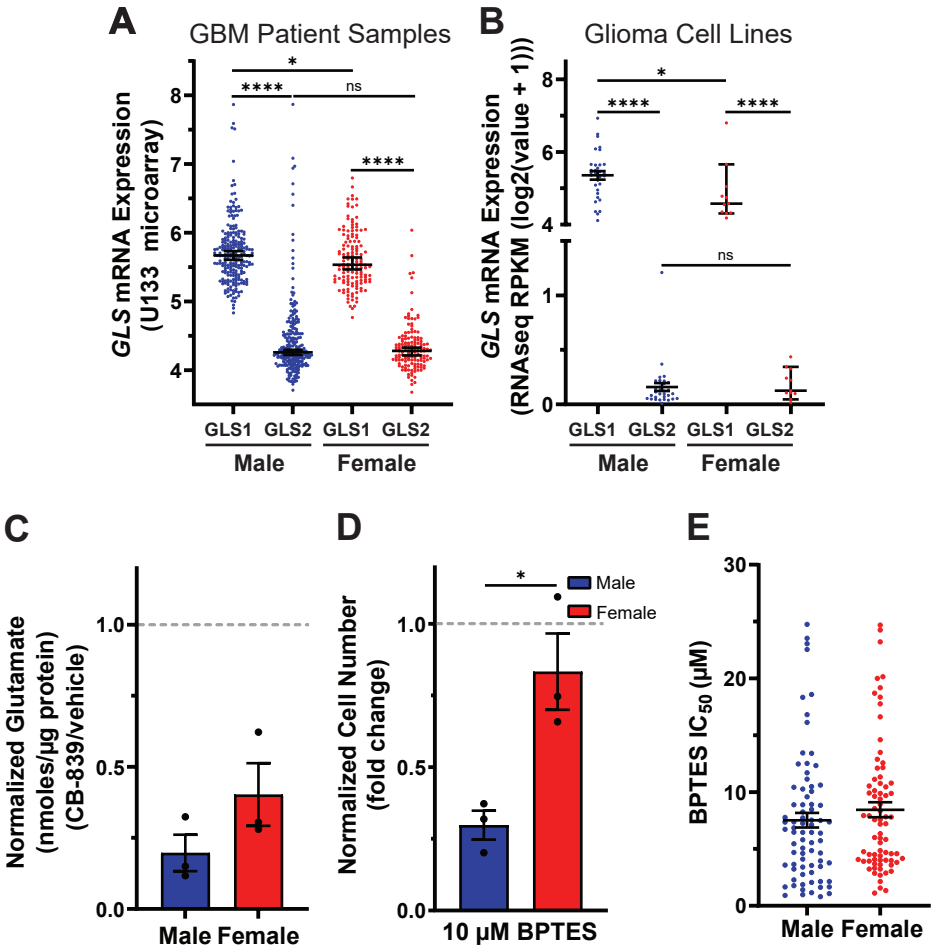

Figure S3. GLS1 expression and dependency are greater in male transformed astrocytes and gliomas, related to Figure 4 A, GLS1 and GLS2 mRNA expression levels in n=232 male and n=139 female IDH wild-type GBM patient samples. Data are median +/- 95% CI. ****p<0.0001; Mann-Whitney test. **B,** GLS1 and GLS2 mRNA expression levels in n=32 male and n=11 female human glioma cell lines. Data are median +/- 95% CI. ****p<0.0001; Mann-Whitney test. **C,** Fold change of cellular glutamate levels of transformed astrocytes treated with CB-839 for 24 hrs. Glutamate levels were measured via targeted GS/MS analysis. Data are mean of n=3/sex and treatment (three independent experiments, one male and female cell line); t-test **D,** Cell number assay of transformed astrocytes treated with BPTES or vehicle. Data are mean +/- SEM of n=3/sex (three independent experiments, one male and female cell line). *p<0.05; t-test. **E,** IC_{50} values of male and female tumor cell lines treated with BPTES for 4 days (data obtained from Daemen et al. [S3]). Data are mean +/- SEM of n=77 male and n=76 female tumor cell lines; t-test.

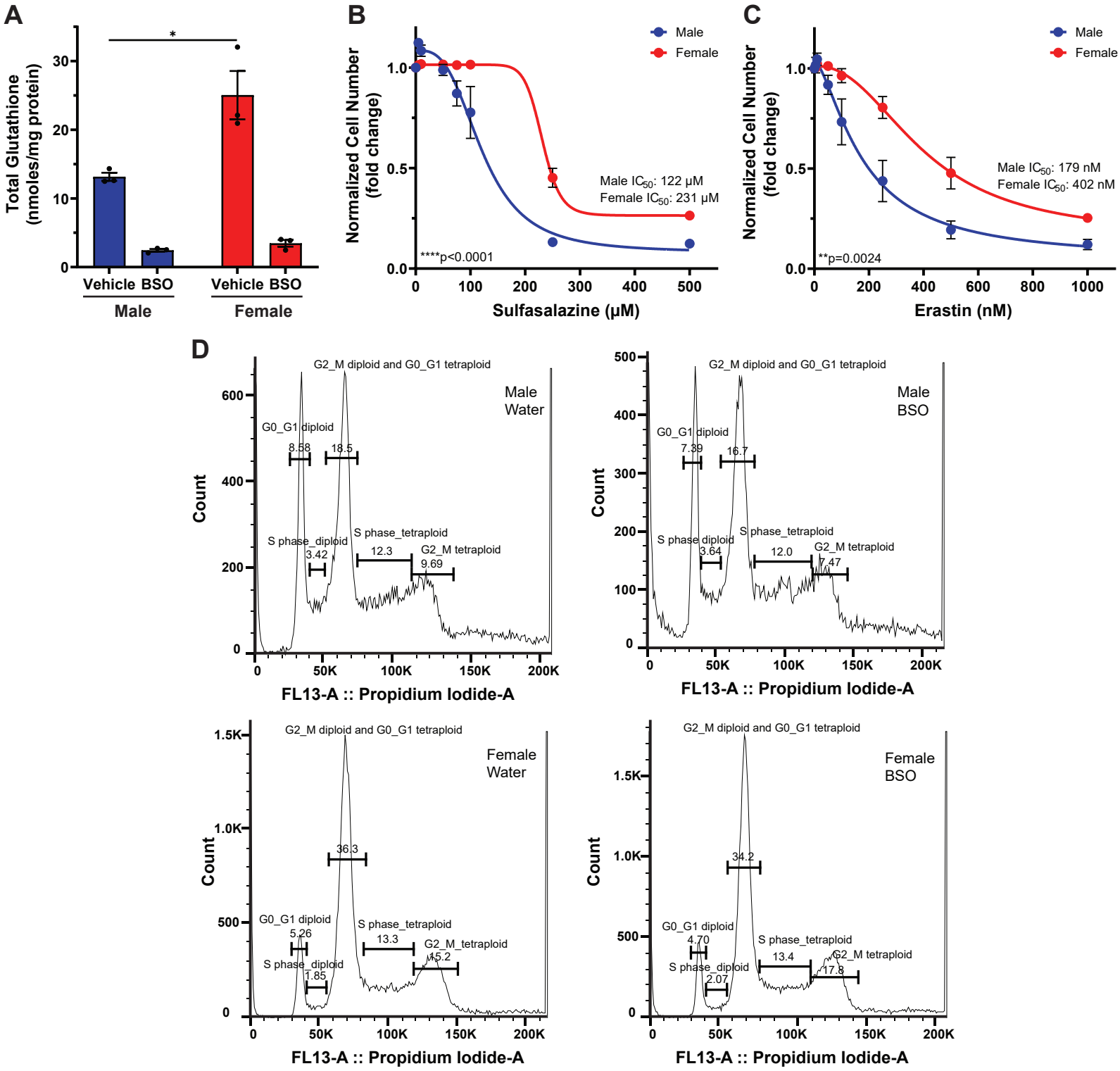
A
Total Glutathione (nmoles/mg protein)
*
Vehicle BSO
Male
Vehicle BSO
Female
B
Normalized Cell Number (fold change)
Male
Female
Male IC50: 122 µM
Female IC50: 231 µM
****p<0.0001
Sulfasalazine (µM)
C
Normalized Cell Number (fold change)
Male
Female
Male IC50: 179 nM
Female IC50: 402 nM
**p=0.0024
Erastin (nM)
D
G2_M diploid and G0_G1 tetraploid
Male Water
G0_G1 diploid 8.58
18.5
S phase_diploid 3.42
S phase_tetraploid 12.3
G2_M tetraploid 9.69
Count
FL13-A :: Propidium Iodide-A
G2_M diploid and G0_G1 tetraploid
Male BSO
G0_G1 diploid 7.39
16.7
S phase diploid 3.64
S phase_tetraploid 12.0
G2_M tetraploid 7.47
Count
FL13-A :: Propidium Iodide-A
G2_M diploid and G0_G1 tetraploid
Female Water
36.3
G0_G1 diploid 5.26
S phase_diploid 1.85
S phase_tetraploid 13.3
G2_M_tetraploid 15.2
Count
FL13-A :: Propidium Iodide-A
G2_M diploid and G0_G1 tetraploid
Female BSO
34.2
G0_G1 diploid 4.70
S phase_diploid 2.07
S phase_tetraploid 13.4
G2_M tetraploid 17.8
Count
FL13-A :: Propidium Iodide-A

Figure S4. Male transformed astrocytes are more dependent on glutathione for redox balance, related to Figure 5 A, Total glutathione levels in transformed astrocytes treated with buthionine sulfoximine (BSO) or vehicle. Data are mean +/- SEM of n=3/sex (three independent experiments, one male and female cell line). *p<0.05; t-test. **B-C,** Sulfasalazine (SAS) **(B)** and erastin **(C)** dose-response curves of transformed astrocytes. Data are mean +/- SEM of n=3/sex (three independent experiments, one male and female cell line). **p=0.0024, ****p<0.0001; two-way ANOVA. **D**, Representative propidium iodide histograms of transformed astrocytes treated with BSO or vehicle. The cell cycle subfractions (G0/G1, S-phase, G2/M) are depicted for the diploid and tetraploid cell populations. Histograms shown are representative examples chosen from three independent experiments.

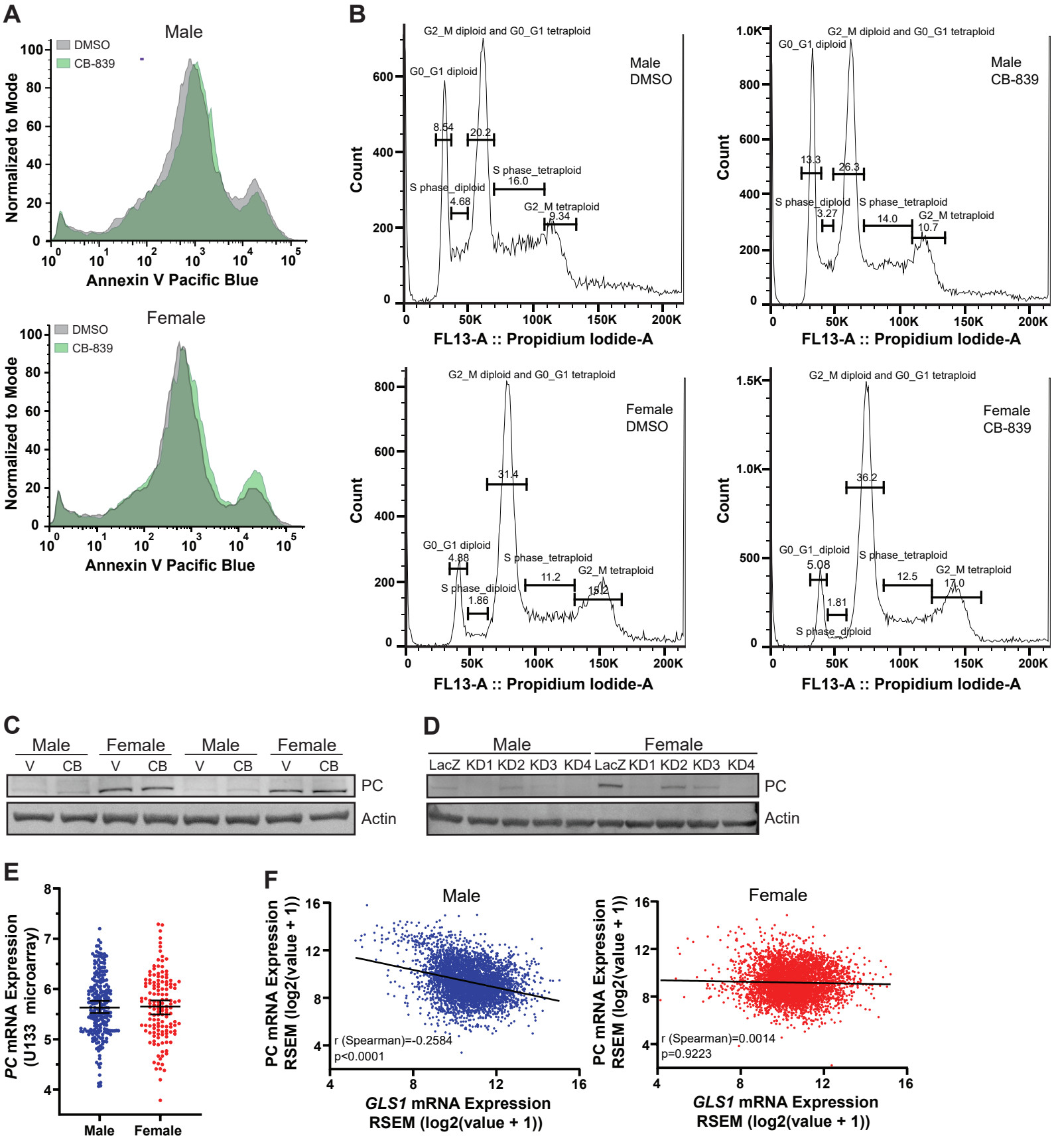
A
Male
DMSO
CB-839
Normalized to Mode
Annexin V Pacific Blue
Female
B
G2_M diploid and G0_G1 tetraploid
G0_G1 diploid
S phase_diploid
S phase_tetraploid
G2_M tetraploid
Male DMSO
Male CB-839
Female DMSO
Female CB-839
Count
FL13-A :: Propidium Iodide-A
C
Male
Female
V
CB
PC
Actin
D
LacZ KD1 KD2 KD3 KD4
E
PC mRNA Expression (U133 microarray)
F
PC mRNA Expression RSEM (log2(value + 1))
r (Spearman)=-0.2584
p<0.0001
r (Spearman)=0.0014
p=0.9223
GLS1 mRNA Expression RSEM (log2(value + 1))

Figure S5. Male transformed astrocytes require glutamine to replenish their TCA cycle, related to Figure 6 A, Representative Annexin V histograms of transformed astrocytes treated with CB-839 or vehicle. Histograms shown are representative examples chosen from three independent experiments. **B,** Representative propidium iodide histograms of transformed astrocytes treated with CB-839 or vehicle. The cell cycle subfractions (G0/G1, S-phase, G2/M) are depicted for the diploid and tetraploid cell population. Histograms shown are a representative example chosen from three independent experiments. **C,** Western blot showing PC expression in transformed astrocytes upon treatment with CB-839 or vehicle from two independent experiments. V=vehicle, CB=CB-839. **D,** Western Blot showing PC expression in transformed astrocyte control cells (LacZ ctrl) and transformed astrocyte PC knockdown cells (PC KD). Western blot shown is a representative blot chosen from three independent experiments. **E,** PC mRNA expression levels in n=232 male and n=139 female IDH wild-type GBM patient samples. Data are median +/- 95% CI; t-test. **F,** Nonparametric Spearman correlation between PC and GLS1 mRNA expression levels in n=4714 male and n=4982 female pan-cancer patient samples.

Table S2. Glioma patient characteristics, related to Figure 2

Characteristic	Female, n = 13[a]	Male, n = 15[a]	Total, n = 28[a]
Age (Average, SD)	45.62, 10.74	56.47, 13.64	51.43, 13.34
Race[b]			
Asian	1 (8%)	1 (7%)	2 (7%)
Black/African American	0 (0%)	1 (7%)	1 (4%)
Other	1 (8%)	1 (7%)	2 (7%)
White	11 (84%)	12 (79%)	23 (82%)
Ethnicity[b]			
Hispanic or Latino	0 (0%)	3 (20%)	3 (11%)
Non-Hispanic	11 (85%)	12 (80%)	23 (82%)
Unknown	2 (15%)	0 (0%)	2 (7%)
Diagnosis			
Anaplastic astrocytoma	3 (23%)	3 (20%)	6 (21%)
Anaplastic ependymoma	1 (8%)	0 (0%)	1 (4%)
Anaplastic oligodendroglioma	2 (15%)	0 (0%)	2 (7%)
Astrocytoma	4 (31%)	0 (0%)	4 (14%)
Glioblastoma	3 (23%)	11 (73%)	14 (50%)
Oligodendroglioma	0 (0%)	1 (7%)	1 (4%)
Grade			
2	4 (31%)	1 (7%)	5 (18%)
3	6 (46%)	3 (20%)	9 (32%)
4	3 (23%)	11 (73%)	14 (50%)
IDH status			
Mutant	8 (62%)	3 (20%)	11 (39%)
WT	5 (38%)	11 (73%)	16 (57%)
Unknown	0 (0%)	1 (7%)	1 (4%)

[a]Statistics presented: n (%)

[b]Self-reported

Table S3. m/z values monitored for glutamine and glucose labeling studies, related to Figure 3 and Figure 6 and STAR★Methods

Metabolite	m/z monitored
GC/MS [$^{13}C_5{}^{15}N_2$]Gln	
Alanine	260.1, 261.1, 262.1, 263.1, 264.1, 265.1, 266.1, 267.1
Fumarate	287.1, 288.1, 289.1, 290.1, 291.1, 292.1, 293.1, 294.1
Valine	288.1, 289.1, 290.1. 291.1, 292.1, 293.1, 294.1, 295.1, 296.1, 297.1
Succinate	289.1, 290.1, 292.1, 293.1, 294.1, 295.1, 296.1
Leucine	302.1, 303.1, 304.1, 305.1, 306.1, 307.1, 308.1, 309.1, 310.1, 311.1, 312.1
Isoleucine	302.1, 303.1, 304.1, 305.1, 306.1, 307.1, 308.1, 309.1, 310.1, 311.1, 312.1
α-Ketoglutarate	346.2, 347.2, 348.2, 349.2, 350.2, 351.2, 352.2, 353.2, 354.2
Serine	390.2, 391.2, 392.2, 393.2, 394.2, 395.2, 396.2, 397.2
Aspartate	418.3, 419.3, 420.3, 421.3, 422.3, 423.3, 424.3, 425.3, 426.3
Malate	419.3, 420.3, 421.3, 422.3, 423.3, 424.3, 425.3. 426.3
Glutamate	432.3, 433.3, 434.3, 435.3, 436.3, 437.3, 438.3, 439.3, 440.3, 441.3
Citrate	591.4, 592.4, 593.4, 594.4, 595.4, 596.4, 597.4, 598.4, 599.4, 600.4
LC/MS [$^{13}C_5{}^{15}N_2$]Gln	
Glutathione (red.)	306.1, 307.1, 308.1, 309.1, 310.1, 311.1, 312.1, 313.1, 314.1, 315.1, 316.1
Glutathione (oxid.)	611.1, 612.1, 613.2, 614.2, 615.2, 616.2, 617.2, 618.2, 619.2, 620.2, 621.2, 622.2, 623.2, 624.2, 625.2, 626.2, 627.2, 628.2, 629.2, 630.2, 631.2
GC/MS [$^{13}C_6$]Glc	
Fumarate	287.1, 288.1, 289.1, 290.1, 291.1, 292.1, 293.1
Aspartate	418.3, 419.3, 420.3, 421.3, 422.3, 423.3, 424.3
Malate	419.3, 420.3, 421.3, 422.3, 423.3, 424.3, 425.3
Citrate	591.4, 592.4, 593.4, 594.4, 595.4, 596.4, 597.4

Table S6. Metabolite ions monitored for targeted GC/MS analysis, related to Figure 4 and STAR★Methods

Metabolites	Ions	Internal Standards (IS)	IS Ions
Alanine	232.1	$^{13}C_3{}^{15}N$ L-Alanine	235.1
Glycine	218.1	$^{13}C_2{}^{15}N$ Glycine	220.1
Valine	186.2	$^{13}C_5{}^{15}N$ L-Valine	191.2
Leucine	200.2	$^{13}C_6{}^{15}N$ L-Leucine	206.2
Isoleucine	200.2	$^{13}C_6{}^{15}N$ L-Isoleucine	206.2
Proline	184.1	$^{13}C_5{}^{15}N$ L-Proline	189.1
Methionine	218.1	$^{13}C_5{}^{15}N$ L-Methionine	223.2
Serine	288.1	$^{13}C_3{}^{15}N$ L-Serine	291.1
Threonine	303.2	$^{13}C_4{}^{15}N$ L-Threonine	306.2
Phenylalanine	302.1	$^{13}C_9{}^{15}N$ L-Phenylalanine	305.1
Aspartate	302.1	$^{13}C_4{}^{15}N$ L-Aspartate	305.1
Cysteine	302.1	$^{13}C_3{}^{15}N$ L-Cysteine	305.1
Glutamate	432.3	$^{13}C_5{}^{15}N$ L-Glutamate	438.3
Asparagine	417.3	$^{13}C_4{}^{15}N_2$ L-Asparagine	423.3
Lysine	300.2	$^{13}C_6{}^{15}N_2$ L-Lysine	307.2
Glutamine	431.3	$^{13}C_5{}^{15}N_2$ L-Glutamine	438.3
Histidine	196.1	$^{13}C_6{}^{15}N_3$ L-Histidine	202.2
Tyrosine	302.1	$^{13}C_9{}^{15}N$ L-Tyrosine	305.1
Tryptophan	302.1	$^{13}C_{11}{}^{15}N_2$ L-Tryptophan	305.1
Cystine	348.2	$^{13}C_6{}^{15}N_2$ L-Cystine	352.2
Pyruvate	174.0	$^{13}C_3$ Pyruvate	177.0
Lactate	261.1	$^{13}C_3$ Lactate	264.1
Citrate	459.3	$^{13}C_6$ Citrate	465.3
α-ketoglutarate	346.1	$^{13}C_4$ α-ketoglutarate	350.1
Succinic acid	289.1	$^{13}C_4$ Succinic acid	293.1
Fumaric acid	287.1	$^{13}C_4$ Fumaric acid	291.1
Malic acid	419.3	$^{13}C_4$ Malic acid	423.3

References

S1 Prabhu, A.H., Kant, S., Kesarwani, P., Ahmed, K., Forsyth, P., Nakano, I., and Chinnaiyan, P. (2019). Integrative cross-platform analyses identify enhanced heterotrophy as a metabolic hallmark in glioblastoma. Neuro. Oncol. *21*, 337–347. doi:10.1093/neuonc/noy185.

S2 Chinnaiyan, P., Kensicki, E., Bloom, G., Prabhu, A., Sarcar, B., Kahali, S., Eschrich, S., Qu, X., Forsyth, P., and Gillies, R. (2012). The Metabolomic Signature of Malignant Glioma Reflects Accelerated Anabolic Metabolism. Cancer Res. *72*, 5878–5888. doi:10.1158/0008-5472.CAN-12-1572-T.

S3 Daemen, A., Liu, B., Song, K., Kwong, M., Gao, M., Hong, R., Nannini, M., Peterson, D., Liederer, B.M., de la Cruz, C., et al. (2018). Pan-Cancer Metabolic Signature Predicts Co-Dependency on Glutaminase and De Novo Glutathione Synthesis Linked to a High-Mesenchymal Cell State. Cell Metab. *28*, 383-399.e9. doi:10.1016/j.cmet.2018.06.003.